ACS APPLIED POLYMER MATERIALS

pubs.acs.org/acsapm Article

Shape-Memory Conductive Hydrogels Featuring Permanent and Temporary Dual-State Programmability

Ping Guo, Jie Zhou, Chengnan Qian, Wenjie Cao, Yang Yu, Lin Cheng, Daoyou Guo, Huaping Wu,* and Aiping Liu*

Cite This: *ACS Appl. Polym. Mater.* 2025, 7, 15659−15670 Read Online

ACCESS | Metrics & More | Article Recommendations | Supporting Information

ABSTRACT: Conductive hydrogels, which possess electrical sensing signaling and deformable capabilities, are considered to be one of the most promising soft materials for the fabrication of artificial intelligence devices such as soft actuators and smart robots. Shape memory conductive hydrogels (SMCHs), characterized by high sensitivity to various external stimuli including pH, heat, light, chemicals, electricity, and magnetism, have emerged as rapidly advancing smart materials in recent years due to their unique capability to transition between a permanent state (steady state) and a temporary state (transient state). However, most commercially available SMCHs can only achieve programmable behavior for a temporary state, which significantly restricts their potential applications in areas such as biomedical devices, soft robotics, and adaptive structures. In this study, we propose a photothermal-responsive, dual-state programmable composite material called a PVA/MXene hydrogel where the programming behavior of both permanent and temporary states is controlled by distinct supramolecular interactions between PVA and MXene. Leveraging the electrical conductivity of MXene, we can monitor the transformation process of the hydrogel and determine its final state (permanent or temporary) via changes in the electrical signal. Additionally, we have developed a multiphysics field simulation model using finite element analysis to demonstrate the spatiotemporal controllability of PVA/MXene hydrogel under near-infrared light irradiation, including local control, unfolding angle modulation, and sequential actuation. The versatility of the PVA/MXene hydrogel is exemplified through applications such as constructing collapsible wings, designing machine grippers, and unfolding battery panels. Furthermore, structural modifications endow the hydrogel with enhanced sensing capabilities, enabling dynamic adjustment of the circuit topology for adaptive electronics. This intriguing work not only presents an alternative approach to MXene-based actuator design but also offers distinctive solutions for the broader field of polymer composite actuators, paving the way for prospects in adaptive structural design and intelligence device fabrication.

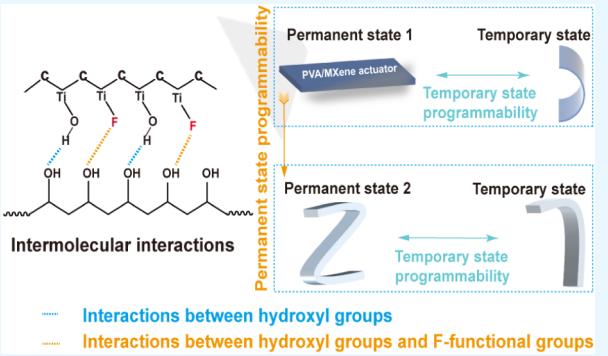

KEYWORDS: *shape memory, conductive hydrogels, dual-state programmability, photothermal driving, strain sensing*

INTRODUCTION

Conductive hydrogels have a wide range of applications in various fields, including flexible sensing, wearable electronics, tissue engineering, electronic skin, soft robotics, and others,[1−3] owing to their adjustable mechanical properties, tissue-like softness, good biological properties, and excellent conductivity.[4−6] Among these applications, hydrogel sensors can accurately convert external deformation into recordable electrical signals and have garnered significant attention from researchers.[7−10] Nevertheless, conductive hydrogels can be singly deformed only by simple external forces such as stretching and bending to give electrical signal changes, which pose substantial challenges for their practical application in complex environments. Shape memory conductive hydrogels (SMCHs) represent a subset of conductive hydrogels capable of converting specific external triggers (e.g., pH, heat, light, chemicals, electricity, and magnetism) into intrinsic mechanical motion.[11−13] These materials employ stimulus-responsive mechanisms to achieve deformation without relying on external mechanical loads or bulky actuation systems such as motors or pneumatic pumps.[14,15] Furthermore, the actuation process can be monitored by electrical signals. Sensitive electrical signals and stimuli-responsive, actuation-capable SMCHs are therefore considered one of the most promising soft materials for the fabrication of artificial intelligence devices, such as soft actuators and smart robots. For instance, Zhao et al.[16] developed a composite hydrogel

Received: September 13, 2025
Revised: October 31, 2025
Accepted: November 5, 2025
Published: November 18, 2025

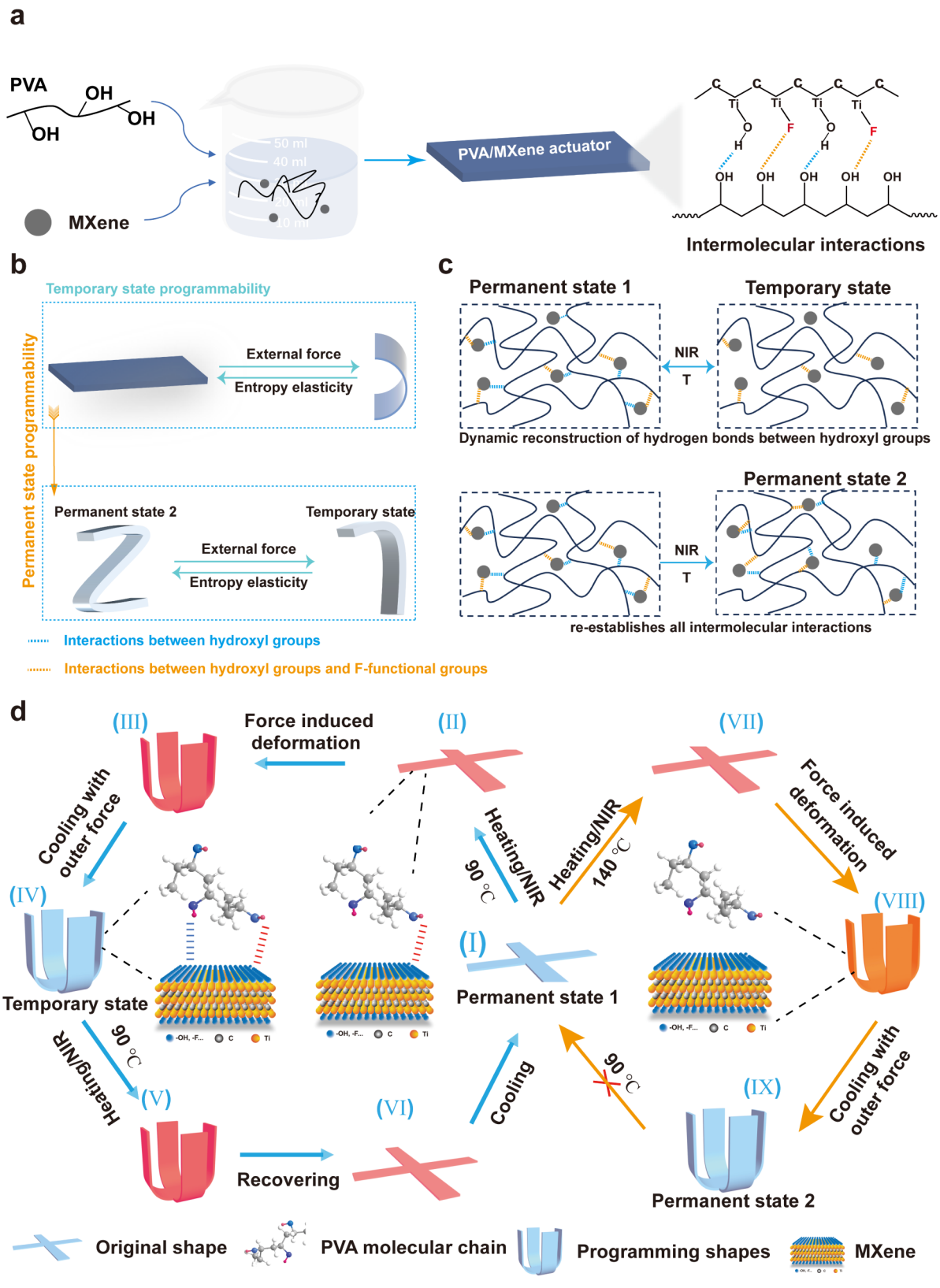

Figure 1. (a) Schematic diagram of the preparation process for the PVA/MXene composite hydrogel. (b) Schematic illustration of the dual-mode programming process in the PVA/MXene composite hydrogel. (c) Evolution of dynamic interactions during the dual-mode programming process. (d) Specific steps for dual-state programming of PVA/MXene composite hydrogels: (I) Permanent state 1 of PVA/MXene. (II) Heating PVA/MXene to 90 °C. (III) Programming a temporary state into PVA/MXene. (IV) Retention of the temporary state upon cooling. (V) Reheating PVA/MXene to 90 °C. (VI) The PVA/MXene transitions from the temporary state back to permanent state 1. (VII) Further heating PVA/MXene to 90 °C. (VIII) PVA/MXene transitions from permanent state 1 to permanent state 2. (IX) Maintenance of permanent state 2 after cooling.

https://doi.org/10.1021/acsapm.5c03453
ACS Appl. Polym. Mater. 2025, 7, 15659−15670

consisting of sea cucumber peptide (SCP) and liquid metal (LM) (SCP/LM). This hydrogel species possesses shape memory functionality, enabling rapid and complex deformations under near-infrared (NIR) irradiation, along with excellent reversibility during temperature variations. Geng et al.[17] fabricated a triple-shape memory effect hydrogel with excellent mechanical properties, used it to construct a bionic dragonfly soft robot, and verified its infrared-responsive shape memory behavior. Although SMCHs exhibit remarkable capabilities in transitioning between stable and transient states, conventional shape memory polymers are restricted to programming only temporary shapes. By enabling the programming of the permanent state, the initial configuration can be redefined without altering the entropic conditions, thus significantly enhancing the controllability of material morphology. Therefore, given that SMCHs possess shape memory functionality, achieving dual-state programmability—both permanent and transient—in SMCHs and recording the state of shape deformation along with its dynamic process through electrical signal variations hold significant research value.

In the midst of external triggers, light with unique propagation properties is regarded as an ideal stimulation source due to its multiple advantages, including instantaneous control, environmental friendliness, and noncontact triggering. Visible and NIR light are particularly preferred trigger sources due to their high energy levels and negligible toxicity in daily life and industrial production.[18] Many photothermal materials, including graphene nanosheets, silver nanowires, carbon nanotubes, and so on, are integrated into the hydrogel system, using their photothermal characteristics to achieve photothermal stimulation-induced actuation.[19−21] Particularly, the emerging two-dimensional material MXene, with remarkable physical and chemical properties, has attracted considerable researchers' interest due to its considerable potential for photothermal conversion (PC) through localized surface plasmon resonance (LSPR).[22−24] Ding et al. introduced MXene into hydrophilic poly(vinyl alcohol) (PVA) to develop photoresponsive hydrogels, modulating interfacial interactions by adjusting the MXene content to precisely control temporary shape programming. However, most existing studies have primarily focused on temporary morphology programming, with limited exploration of permanent morphology programming in SMCHs. Additionally, there is insufficient consideration of information feedback and environmental interactions during deformation, which significantly restricts their potential applications in fields such as biomedical devices, soft robotics, and adaptive structures.

In this study, a conductive composite hydrogel based on PVA/MXene was successfully prepared. This material can regulate the intermolecular interactions within it in response to temperature and near-infrared (NIR) light, enabling photothermally triggered shape memory behavior and demonstrating excellent dual-state programmability in both permanent and transient configurations. Furthermore, its inherent high electrical conductivity provides reliable sensing performance. This distinctive dual-state programmable capability with self-sensing capacity presents significant potential for applications requiring highly adaptive and reconfigurable structures.

RESULTS AND DISCUSSION

Design Strategy for Two-State Programmable PVA/MXene Hydrogel. The etching process usually results in multiple functional groups onto the MXene surface, including F-functional groups and hydroxyl groups,[25] as illustrated in Figure 1a. This modification leads to two distinct types of supramolecular interactions within the PVA/MXene composite.[26]

As shown in Figure 1b, the PVA/MXene composite hydrogel is first programmed under an external force and subsequently undergoes an entropy-driven elastic recovery upon thermal stimulation. The microscopic mechanism underlying this macroscopic behavior is revealed in Figure 1c, which illustrates the dynamic interactions and reversible reconstruction between PVA molecular chains and MXene nanosheets during the dual-mode programming process. Specifically, the weaker hydrogen bonding between the hydroxyl groups of PVA and MXene is responsible for the temporary state shape memory function of PVA/MXene; namely, the formation and dissociation of these dynamic hydrogen bonds permit the material to remain in a temporary state. Consequently, PVA/MXene can be programmed from a strip-shaped (permanent state 1) configuration into a C-shaped configuration (temporary state) by precise temperature and external force control. In contrast, the stronger interactions between the F-functional groups on MXene and the hydroxyl groups on the PVA molecular chain allow for the superior programming of the permanent state for PVA/MXene. Furthermore, by applying higher temperature and external force, the strip-shaped PVA/MXene can be programmed into a Z-shaped structure (permanent state 2). Notably, PVA/MXene with a Z-shaped structure also exhibits temporary state programming capabilities. For example, the Z-shaped structure can be reprogrammed into a 7-shaped configuration.

In conjunction with paper-cutting technology, PVA/MXene is fabricated into a cross-shaped structure, incorporating a dual-state programming process. The intrinsic mechanisms underlying this dual-state programming are thoroughly investigated. As shown in Figure 1d, Figures I−VI elucidate the programming pathways of the temporary states. Initially, in PVA/MXene (Figure I), numerous intermolecular hydrogen bonds form between the surface functional groups of MXene and the PVA molecular chains. These interactions include hydrogen bonding between the hydroxyl groups of MXene and PVA, as well as strong interactions between the F-functional groups of MXene and the hydroxyl groups of PVA. In this state, the PVA/MXene system reaches thermodynamic equilibrium with lower entropy,[27,28] thereby constraining the mobility of the PVA molecular chains.[29] Upon exposure to temperature or NIR stimulation, the hydrogen bonds between the hydroxyl groups of PVA and MXene dynamically dissociate, weakening these interactions (Figure II).[30] This transition leads to a highly entropic state for the PVA molecular chains, enabling PVA/MXene to assume a different shape in response to external forces (Figure III). Upon cooling, the hydrogen bonds between the hydroxyl groups of PVA and MXene are dynamically reconstructed, allowing PVA/MXene to maintain the programmed shape (Figure IV). Upon reheating (Figure V), the hydrogen bonding interactions weaken again, causing PVA/MXene to revert to its initial shape due to the entropic elasticity of the PVA molecular chains (Figure VI). Further cooling to room temperature restores the intermolecular interactions, bringing PVA/MXene back to its thermodynamic steady state. The process of programming the permanent state is examined in depth in Figures I and VII−IX. Similarly, when the temperature reaches 140 °C (Figure VII),

https://doi.org/10.1021/acsapm.5c03453
ACS Appl. Polym. Mater. 2025, 7, 15659−15670

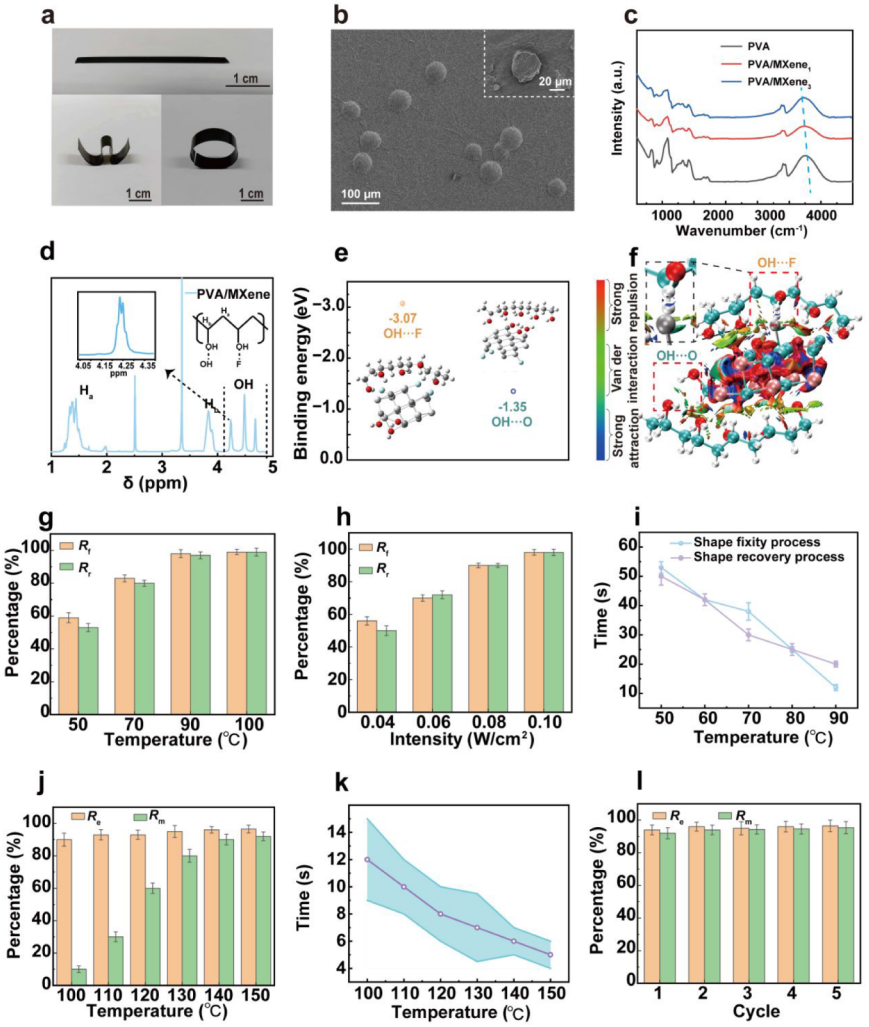

Figure 2. (a) Experimental demonstration of programming PVA/MXene hydrogels into diverse shapes. (b) SEM images of PVA/MXene composite hydrogel with 3 wt % MXene. (c) FTIR spectra of PVA/MXene composite hydrogels with varying MXene contents. (d) ^{1}H-NMR spectrum of PVA/MXene in DMSO-d6 solvent. (e) The binding energy of the PVA/MXene system. (f) The noncovalent interaction of the PVA/MXene system is based on VMD software. (g) Shape memory effect of PVA/MXene hydrogels at different temperatures. (h) Shape memory effect of PVA/MXene hydrogels under different NIR light intensities. (i) Time-dependent morphological changes in temporary shape programming of PVA/MXene hydrogels at different temperatures. (j) Effect of permanent state programming based on PVA/MXene at different temperatures. (k) Influence of temperature on the programming of the permanent state in PVA/MXene hydrogels. (l) Temporary state programming loop for permanent state 2 of PVA/MXene hydrogel.

the hydrogen bonds between the PVA and MXene hydroxyl groups partially dissociate, leading to a decrease in the strength of these interactions. Notably, at this temperature, the external environment provides sufficient energy to disrupt the strong interaction between the F-functional groups of MXene and the hydroxyl groups of PVA.[31] Consequently, the permanent state of PVA can be programmed (Figure VIII). Upon removal of the energy source (NIR/temperature), the natural cooling process re-establishes all intermolecular interactions, resulting in a thermodynamic equilibrium (Figure IX). The permanent state of the PVA/MXene hydrogel is successfully programmed, transforming its configuration from cross-shaped to flower-shaped.

Photothermal Conversion Properties and Dual-State Programmability of PVA/MXene Hydrogels. These two interaction mechanisms, with significant differences, endow PVA/MXene hydrogels with the ability for dual-state programming. Figure 2a shows the shape-programming capability of PVA/MXene, demonstrating how straight strips can be programmed into the shapes of letters W and O. For example, a PVA/MXene hydrogel with a strip shape is programmed into another shape when heated to 90 °C, and when the temperature returns to room temperature, the PVA/MXene hydrogel retains the O-shape (temporary state). Given the critical role of MXene in this process, ensuring a homogeneous dispersion of MXene is essential. As shown in the SEM image in Figure 2b, the MXene nanosheets exhibit a characteristic two-dimensional (2D) layered structure and are homogeneously dispersed within the gel matrix. Some wrinkled MXene nanosheets are clearly visible in the PVA/MXene composite, especially when the mass percentage of MXene increases to 4% due to MXene agglomeration (Figure S2). In addition, the elemental distribution was analyzed using EDX spectroscopy, and it is clearly observed that PVA contains only C and O elements, while F and Ti are present and uniformly distributed in the PVA/MXene samples (Figure S3). Furthermore, the FT-IR spectra of PVA/MXene (Figure 2c) reveal a red shift of the hydroxyl peak of PVA as the MXene

https://doi.org/10.1021/acsapm.5c03453
ACS Appl. Polym. Mater. 2025, 7, 15659−15670

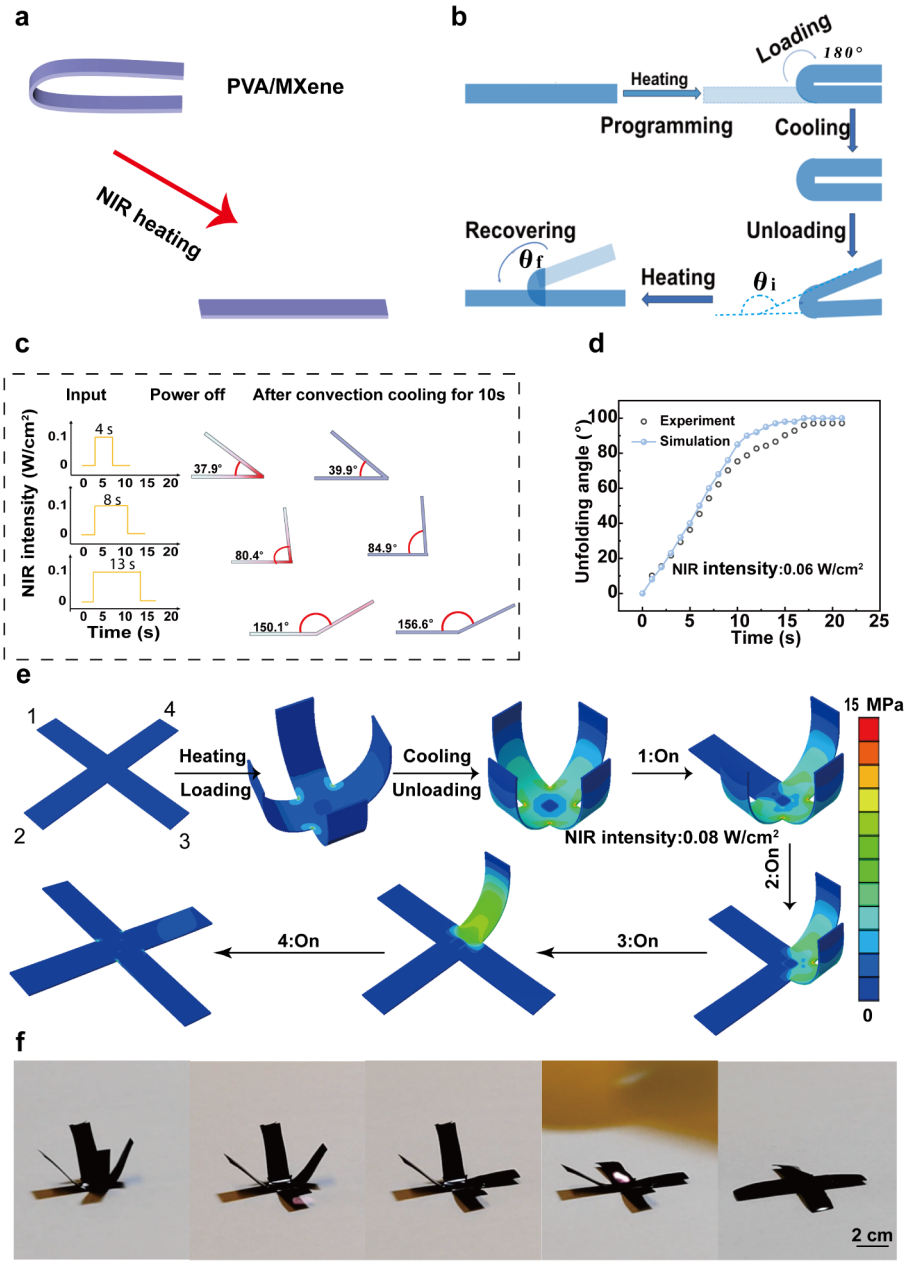

Figure 3. (a) Schematic illustration of the angular unfolding process of the U-shaped structure. (b) Experimental setup and methodology for controlling the unfolding angle. (c) Unfolding angles of PVA/MXene at varying durations of near-infrared (NIR) irradiation, followed by 10 s of convective cooling. (d) Correlation between NIR heating duration and resultant angle. (e) Finite element analysis (FEA) for shape transformation mechanics. (f) Sequential snapshots capturing the shape-shifting process.

content increases, indicating incremental supramolecular interactions between PVA and MXene. Nuclear magnetic resonance (NMR) spectra confirmed this, in which the characteristic peak of the hydroxyl group showed a phenomenon of multiple peaks, indicating that the hydroxyl group of PVA was affected by different hydrogen bond strengths (Figure 2d).[32] Subsequently, the molecular structure of PVA/MXene was optimized by using Gaussian software. Noncovalent interaction (NCI) analysis was then performed utilizing Multiwfn 3.8.[33] As illustrated in Figure 2e, the calculated binding energy for the PVA/MXene system reached −3.07 eV when interactions occurred between the −F functional groups on the MXene surface and the −OH groups of PVA. In contrast, interactions between the −OH groups on MXene and PVA's −OH groups yielded a significantly higher binding energy of −1.07 eV. This pronounced difference indicates stronger hydrogen bonding between the MXene's −F groups and PVA's −OH groups, leading to enhanced stability reflected by the lower binding energy. To provide a more intuitive representation, we employed VMD software to visualize the weak interactions within the system. The distinct color differences observed further confirm the presence of two types of hydrogen bonds with differing strengths, consistent with the calculated binding energies (Figure 2f).

The photothermal conversion characteristics of MXene are key to achieving dual-state programmability of materials. As shown in Figure S4, samples without MXene do not respond to NIR. The equilibrium temperature of the samples

https://doi.org/10.1021/acsapm.5c03453
ACS Appl. Polym. Mater. 2025, 7, 15659−15670

containing MXene increased with the increase of MXene mass fraction under the same light intensity (0.04 W/cm^2), confirming its excellent photothermal performance. It is worth noting that the same equilibrium temperature is maintained after five heating and cooling cycles, demonstrating highly repeatable photothermal stability. In addition, we also investigated the dual-state programming capability of PVA/MXene under both temperature and infrared light stimulation. The programming efficiency of temporary shapes exhibits strong temperature dependence (Figure 2g). At 50 °C, fixation (R_f) and recovery (R_r) ratios are low, while 90 °C yields near-complete programming (R_f = R_r = 98%). NIR irradiation (Figure 2h) achieves similar effects via MXene's photothermal conversion. Performance improves with intensity: R_f is 58% at 0.04 W/cm^2 and exceeds 90% at higher intensities, correlating with increased heat generation. Cyclic stability under thermal/NIR stimuli remains excellent (R_f, R_r > 95%; Figure S5). Programming and recovery times decrease with increasing temperature (Figure 2i) or NIR intensity (Figure S6). Specifically, at 90 °C, the time required to complete shape programming is only 16 s. Similarly, temperature also promotes the recovery process of the hydrogel. Recovery achieves 98% completion within 4 s at 0.1 W/cm,^{2} with a deformation speed of 35°/s. However, at a lower intensity of 0.04 W/cm,^{2} the process is slower and the recovery ratio declines, as the energy supplied is insufficient to disrupt intermolecular interactions.[34] The low temperature also cannot achieve the desired programming effect of the temporary state (Figure S7). In addition, the hydrogel is prepared by evaporation at 40 °C and 60% humidity, and its initial water content is relatively low, approximately 26%. This intrinsic property significantly minimizes water loss at elevated temperatures, thereby ensuring stable performance during the actuation process. A similar law is also obtained for the temperature-dependent transition time from the temporary state to the permanent state, namely, shorter recovery time and higher recovery rate at higher temperature simulation. Permanent state programming was quantified via the shape editing ratio (R_e, analogous to R_f) and maintainability ratio (R_m). R_e exceeds 90% between 100 and 150 °C, but effective permanent programming (R_m > 90%) requires temperatures >140 °C (Figure 2j). Programming time decreases with temperature, reaching 5s (Figure 2k). The hydrogel demonstrates excellent reproducibility in permanent shape programming (Figure 2l), even when reconfigured into complex geometries (Figure 1b), highlighting its potential for adaptive structures.

Next, we also investigated the ability of PVA/MXene to program a permanent state under temperature and infrared light stimulation. In the case of programming permanent shape states, two key parameters were redefined, namely the shape editing ratio (R_e) and the shape maintainability ratio (R_m). The R_e is analogous to the R_f, while the R_m represents the proportion of the shape that can be maintained at 90 °C after programming the PVA/MXene into another shape. As illustrated in Figure 2j, the R_e exceeds 90% within the temperature range of 100−150 °C. However, the R_m reaches 90% only when the temperature exceeds 140 °C. These data indicate that PVA/MXene can effectively program its initial shape at temperatures above 140 °C. As the temperature increases, the time required to program the permanent state of the material decreases, with the minimum programming time being 5 s (Figure 2k). The excellent reproducibility of PVA/MXene's permanent state programming is observed (Figure 2l), even when it is programmed into other shapes (Figure IX), offering PVA/MXene a promising application for adaptive structure design and fabrication.[35]

Finite Element Analysis of Shape Memory Process in PVA/MXene Hydrogels. The shape memory process to precisely control PVA/MXene was further finite-element analyzed by developing a multiphysics field simulation model via the ABAQUS software. The PVA/MXene enables the regulation of the unfolding angle via NIR irradiation (Figure 3a). Figure 3b presents the experimental setup for controlling the unfolding angle. Initially, the flat PVA/MXene is folded into a U-shape (180°), with one edge fixed and the other free to move. The precision of IR control is demonstrated by measuring the change in angle over time. Under constant NIR light (0.1 W/cm^2), different irradiation times result in varying unfolding angles (Figure 3c). For instance, after 4 s of irradiation, the unfolding angle reaches 37.9°, stabilizing at 39.9° after 10 s of natural convective cooling. After 8 s of irradiation, the final unfolding angle of PVA/MXene reaches 84.9°, and after 13 s, it reaches 156.6°. Figure 3d illustrates the predicted unfolding angles from the simulation for varying NIR exposure times, validating the model's accuracy by comparing its predictions with the experimental data. At higher temperatures (80−100 °C), the experimental value is slightly lower than the simulated value, mainly due to heat loss (such as heat convection and heat radiation) during the experiment. This precise control allows PVA/MXene to be fixed at any desired unfolding angle, with continued NIR irradiation leading to further expansion until full opening. This capability enables localized, sequential, and overall deformation control.[36] Figure 3e demonstrates the controlled process of complex deformation through finite element analysis, exemplified by a crucifix shape. The process consists of three stages: 1) overall heating and programming of external forces; 2) cooling and unloading of external forces; and 3) selective localized irradiation by NIR to achieve 90° unfolding of each petal. This approach enables the independent and precise heating of specific petals at different times, eliminating the need for synchronization with other petals. Additionally, a wide range of stress variations is crucial for the shape memory effect. The significant stress generated during the cooling process is responsible for maintaining the temporary shape. Upon reheating, this stress is substantially reduced, thereby facilitating the shape recovery process. The temperature changes during the controlled deformation are illustrated in Figure S8. The experimental snapshots (Figure 3f) and accompanying movie (Movie S1) further validate the accuracy of the multiphysics field model.

Strain Sensing Performance of PVA/MXene Hydrogels. It is well established that MXene, with its considerable specific surface area, excellent hydrophilicity, and high conductivity, has emerged as an optimal candidate for enhancing the conductivity of hydrogels. The incorporation of MXene not only endows the material with photothermal conversion capabilities but also enables it to function as a sensor. Since the strain-sensing range of hydrogels depends on their mechanical properties,[37] the maximum stress and elongation at break of each sample were evaluated under a stretching rate of 50 mm/s. As illustrated in Figure S9, the mechanical properties of PVA/MXene composite hydrogels were optimized by adjusting the mass percentage of MXene. Under optimal conditions, the maximum fracture rate of the PVA/MXene hydrogel can reach 310%. Although this hydrogel

https://doi.org/10.1021/acsapm.5c03453
ACS Appl. Polym. Mater. 2025, 7, 15659−15670

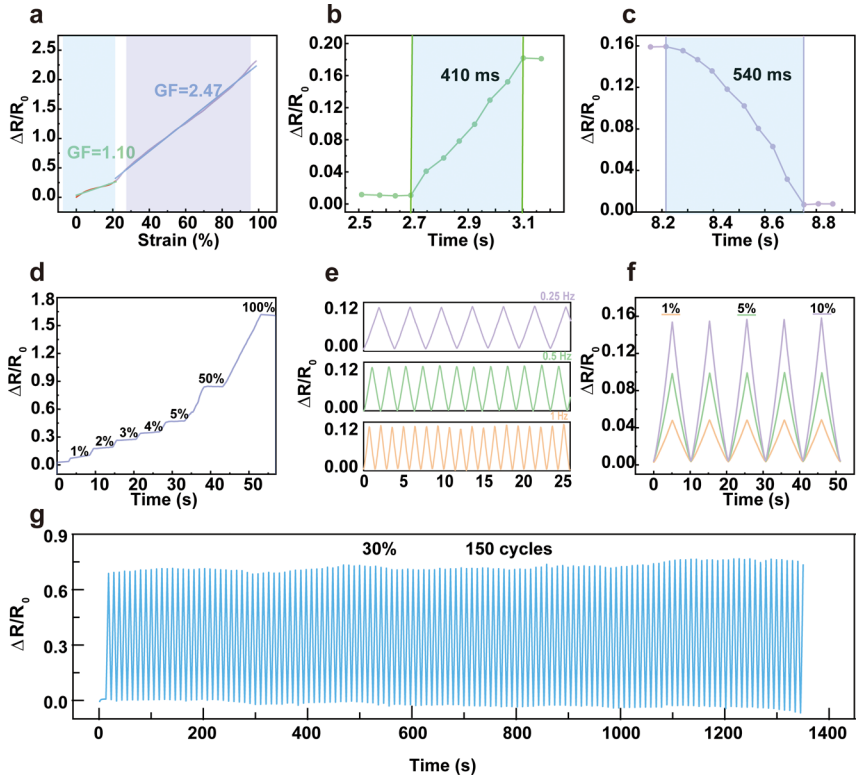

Figure 4. (a) The relationship between strain and relative resistance. (b) Response time of the PVA/MXene sensor. (c) Recovery time of the PVA/MXene sensor. (d) Relative resistance variation under stepwise strains. (e) Relative resistance variation at different frequencies. (f) Repeatability of relative resistance variation at different strains. (g) Long-term stability of the sensor over multiple cycles at 30% strain.

can withstand higher strain, excessive stretching can cause irreversible damage to its microstructure, thereby leading to unstable sensitivity and poor repeatability. To ensure the reliability and repeatability of the data, the upper limit of the analysis strain is set at 100%. Figure 4a illustrates the corresponding sensitivities for different strain ranges; the gauge factor (GF) for the 0−20% strain range is 1.10, while the sensitivity for the 20−80% strain range is 2.47. This discrepancy can be attributed to the distinct response mechanisms involved in structural changes in the conductive network due to the relative slip of the MXene sheets. In the initial stages of small strain, the relative displacement of MXene sheets is relatively minimal, allowing electrons to pass through the breakpoints of the conductive network via the tunneling effect, resulting in a small resistance change. As the strain increases, the conductive network constructed by MXene becomes increasingly disrupted, leading to greater obstruction of electron transport. Consequently, this results in a significant increase in resistance and a higher gauge factor. In addition, response time serves as a critical metric for assessing sensor performance. As presented in Figure 4b and c, the sensor exhibits a rapid response time of 410 ms and a relaxation time of 540 ms when subjected to 1% strain at a high stretching rate of 1000 mm/min. To further substantiate the stability of the electrical signal output by PVA/MXene in response to strain variations, a step diagram of the electrical signal was constructed. Distinct electrical signal values are generated, corresponding to varying strains and frequencies (Figure 4d and e), demonstrating excellent signal reproducibility during five tensile cycles under different strain conditions. As the strain step size increases from 1% to 5% at 1% increments, the resistance correspondingly increases, with the responses of the two cycles being nearly identical. Similarly, when the frequency is increased from 0.25 to 1 Hz, a repeatable and reversible response is observed. The PVA/MXene sensor exhibits a repeatable and strain-dependent resistance response over three cyclic stretches at fixed strains of 1%, 5%, and 10% (Figure 4f). The electrical signals exhibit robust cyclic stability over 100 stretch-release cycles performed under 30% strain (Figure 4g). The slight increase in resistance observed in the final testing phase may be attributed to the potential irreversible breaking of some hydrogen bonds during deformation, likely resulting from polymer chain slippage.[38]

Exquisite Structural Design and Actuation Behavior of PVA/MXene Hydrogels. The PVA/MXene hydrogel, with its unique dual-state programmable properties and spatiotemporal controllability, presents unprecedented opportunities for innovative aircraft wing design. As a demonstrative example, we introduce a precisely controlled photothermal responsive wing origami with variable thickness. The folding and unfolding principles from the art of origami inspire the wing design, enabling the creation of complex structures with variable thickness through the strategic folding and fixing of PVA/MXene material in a crest/trough pattern (Figure 5a). Specifically, peak A regulates the expansion, while peak B controls the contraction. As illustrated in Figure 5b, we program the temporary state of the strip hydrogel to form a wave crest (A_0−A_1). Furthermore, we can control the horizontal extension of the hydrogel via external stimuli such as temperature or near-infrared (NIR) light. Notably, PVA/MXene hydrogels exhibit dual-state programmability. Consequently, we set its permanent state at higher temperatures, transitioning the permanent state from A_0 to B_0. Similarly, we programmed the temporary state of B_0 to form a wave trough.

https://doi.org/10.1021/acsapm.5c03453
ACS Appl. Polym. Mater. 2025, 7, 15659−15670

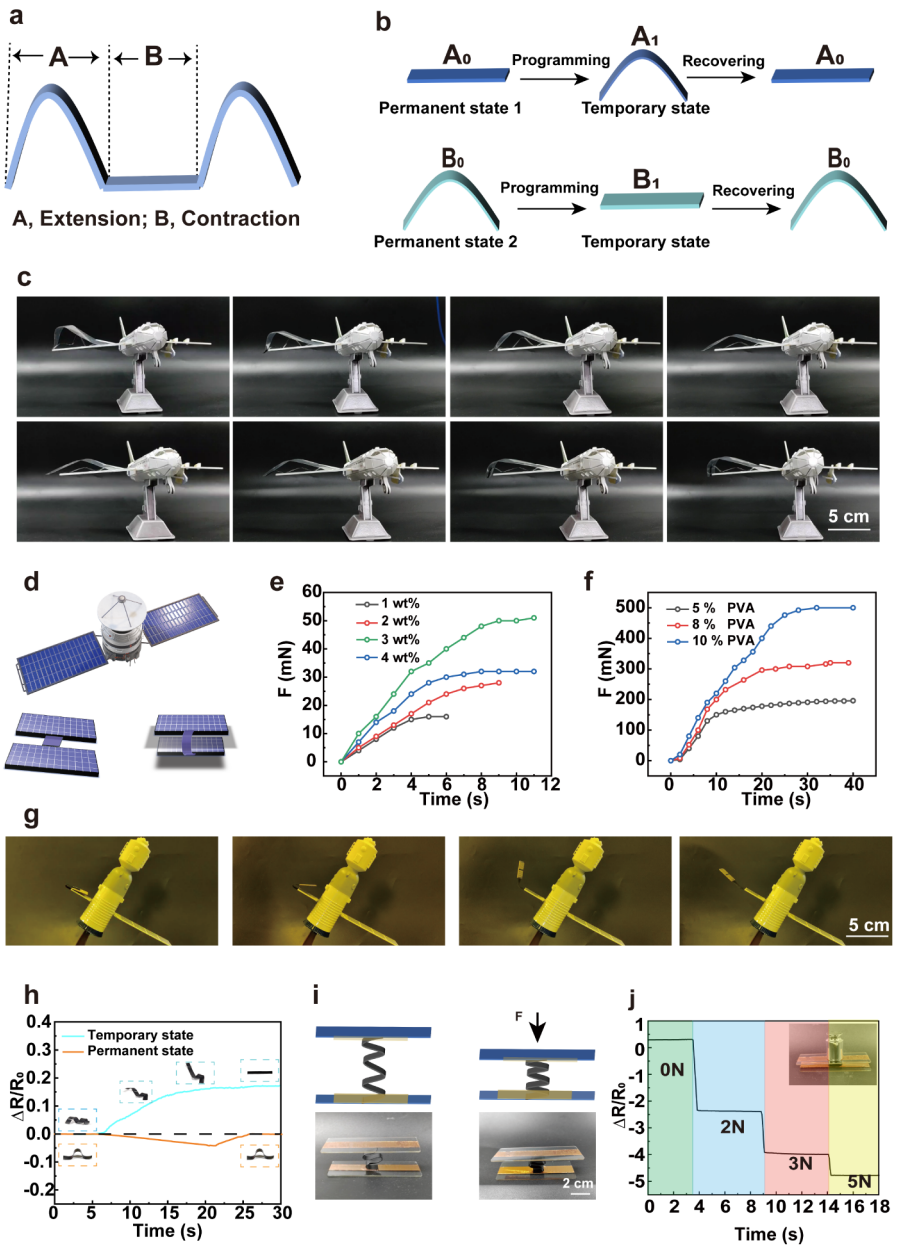

Figure 5. (a) Actuator unit for a variable wing. A controls the expansion process, while B controls the contraction process. (b) Two-state programming controls the actuating process. (c) Snapshots illustrating changes in wing profile shape. (d) Expanded view of battery panel layout. (e) Relationship between varying MXene contents and actuation forces. (f) Influence of different PVA contents on actuation forces. (g) Snapshot of solar panel deployment process. (h) PVA/MXene exhibits temporary state programming by forming a spiral shape. (i) Structural transformation enhances sensing performance. (j) Relative resistance change as a function of applied pressure.

Upon exposure to an external stimulus, B_1 reverts to the original shape of B_0, thereby controlling the hydrogel to contract horizontally. The shape and thickness changes in the wing are clearly depicted in Figure 5c and Movie S2 under NIR radiation. The precise spatiotemporal control of PVA/MXene materials allows for localized or global adjustments, enabling independent modification of distinct sections of the wing to achieve intricate geometries tailored to specific flight requirements and environmental conditions. A similar application is also illustrated in Figure 5d, where PVA/MXene is used for the deployment of solar panels. The initial design allows the panel to be folded in a compact configuration, thereby conserving space. Upon positioning, the panel can be remotely unfolded via infrared radiation (Figure 5g and Movie S3). Furthermore, three PVA/MXene grippers are integrated into an industrial robotic arm, enabling precise gripping, movement, and release of objects (Figure S10). The actuation force generated by MXene increases with higher MXene content until it reaches a peak at 3 wt % (Figure 5e), after which it decreases due to the inhomogeneity caused by excessive MXene. Similarly, when the mass fraction of the PVA exceeds 10%, the system viscosity becomes too high, leading to further inhomogeneity and an actuation force decrease (Figure 5f). The effects of PVA and MXene contents on the driving force were simulated via the response surface method (Figure S11). The results show that when the MXene content is 3 wt %, the maximum driving force is 500 mN, and the corresponding actuation strength is 166 kPa. Based on the superior sensing capability of PVA/MXene,

https://doi.org/10.1021/acsapm.5c03453
ACS Appl. Polym. Mater. 2025, 7, 15659−15670

electrical signals can effectively reflect the two-state programming process. As illustrated in Figure 5h, PVA/MXene exhibits temporary state programming by forming a spiral shape. Under thermal stimulation at 90 °C, the spiral gradually unfolds, accompanied by a gradual increase in the relative resistance. In contrast, when PVA/MXene undergoes permanent state programming to form an arch bridge shape, its structure remains stable under the same temperature conditions (90 °C), with only a slight decrease in relative resistance due to the enhanced electrical conductivity of MXene at elevated temperatures. Notably, the programmable nature of PVA/MXene enables versatile structural configurations, which often correlate with enhanced sensing capabilities. Placing PVA/MXene on a heating platform at 140 °C for several minutes allows it to be rapidly programmed into a snake-like shape. Furthermore, when a straight, strip-like hydrogel is programmed to form a spring-like structure and sandwiched between conductive copper tapes to create a compression sensor (Figure 5i), the spring-like configuration enhances the detection of positive pressure. This is attributed to the rapid increase in the contact area between MXene sheets under pressure, leading to a decrease in resistance (Figure 5j). To evaluate its performance, we conducted a comparative analysis of this work with representative shape-memory hydrogel actuators reported recently.[16,39−43] As shown in the radar image (Figure S12), the PVA/MXene composite hydrogel actuator achieves balanced integration in multiple key performances, including short programming time, fast deformation response, dual-state programming capability, and integrated sensing function. This comprehensive advantage makes the device a highly competitive multifunctional platform, which is expected to be applied in the next generation of soft actuators, wearable electronic devices, and intelligent sensing systems.

CONCLUSION

In conclusion, a PVA/MXene composite hydrogel with dual programming capability for both permanent and temporary states was designed. The mechanism underlying this dual-state programming can be attributed to the dynamic process of hydrogen bonding between the hydroxyl groups of PVA and MXene, and the strong interaction between the F-functional groups of MXene and the hydroxyl groups of PVA, enabling the programming of a temporary state and a permanent state, respectively. The incorporation of MXene not only endows the composites with photothermal conversion capabilities but also significantly enhances their functionality as sensors by enabling the use of electrical signals to accurately reflect the two-state programming process. The dual-state programmability and spatiotemporal controllability of the material have been demonstrated in various applications, including the design of wings and machine grippers. Additionally, structural modifications can alter the sensing mechanism to enable sensing capabilities. The dual-state programmability significantly enhances shape controllability and broadens the material's promising applications in smart materials, particularly in flexible actuators and soft robotics.

EXPERIMENTAL SECTION

Materials. Poly(vinyl alcohol) (PVA 1799), hydrochloric acid (HCl), and lithium fluoride (LiF) were purchased from Shanghai Aladdin Company. Ti_3AlC_2 was purchased from Shanghai Macklin Company.

Preparation of the PVA/MXene Composite Hydrogel. The PVA/MXene composite hydrogels were prepared via a straightforward solution casting process, as illustrated in Figure S1. MXene was first synthesized via the etching of Ti_3AlC_2 powders using LiF/HCl, as detailed in the referenced literature.[44] Specifically, 1.98 g of PVA was dissolved in 20 mL of water in a beaker and heated to 90 °C for 2 h. Following this, 2 mL of MXene dispersion (10 mg/mL) was gradually added while stirring continuously. The resultant PVA/MXene mixture was then poured into a PTFE mold and allowed to dry through water evaporation at 40 °C and 60% humidity, yielding the MXene-based shape memory material. By adjusting the percentage of MXene in the hydrogel from 1 wt % to 4 wt %, the sample was correspondingly defined as PVA/$MXene_y$ (y = 1, 2, 3, and 4).

Characterization Methods. The surface of the PVA/MXene hydrogel samples, which were quenched in liquid nitrogen and subsequently coated with gold, was examined by using scanning electron microscopy (SEM, S-4800, Hitachi, Tokyo, Japan). The ultrasonically dispersed MXene solution was also analyzed via SEM to evaluate its microscopic morphology. Energy Dispersive X-ray (EDX) spectroscopy was used to assess the elemental distribution in the materials. Fourier transform infrared (FT-IR) spectra of PVA/MXene hydrogels were recorded within the range of 4000 to 400 cm^{-1} using a Nicolet Nexus 670 FT-IR spectroscope (Nicolet Instrument Co., USA). Hydrogel samples were trimmed into dimensions of 30 × 10 × 0.3 mm for tensile testing on a universal testing machine. The electromechanical performance of the hydrogel sensors was evaluated in real time using a Keithley 2400 dual-probe measurement system. The measurement was conducted in a two-wire (dual-probe) DC mode with a constant applied voltage of 1.0 V. The resulting current was recorded, and the resistance was calculated using Ohm's law. Temperature stimulation was provided by using a constant-temperature heating table (model 9NBO). NIR light at 808 nm was generated by a laser, and the temperature changes in the hydrogel were monitored with an infrared camera. The entire actuation process was recorded by using a camera. Images at different time points were captured, and the bending angle of the composite actuator was quantified by using ImageJ software. The initial mass of the original hydrogel (m_0) was recorded, followed by subjecting it to an 80 °C oven for 48 h and recording its final mass (m_1). The water content was quantified using the formula:wt % = $(m_0 - m_1)/m_0 \times 100\%$.

The shape memory properties of the PVA/MXene hydrogels were quantified by means of bending tests, which were used to assess the programming characteristics of the permanent and temporary states. Specifically, the flat PVA/MXene hydrogel was first heated at 90 °C for 5 min and then bent to 180° under an external force while maintaining this external force during cooling to room temperature. Subsequently, the temporarily bent hydrogel film with the bent angle of θ_i was reheated at 90 °C, and the change in bending angle (θ_f) over time was recorded. The shape fixity ratio (R_f) and the shape recovery ratio (R_r) of the PVA/MXene hydrogel were defined by the following eqs 1 and 2:[45]

$$R_f = \frac{\theta_i}{180} \times 100\% \quad (1)$$

$$R_r = \frac{\theta_i - \theta_f}{\theta_i} \times 100\% \quad (2)$$

A similar method was applied to evaluate the permanent state programming capability of the PVA/MXene hydrogels. Initially, the flat PVA/MXene hydrogel was heated at 140 °C for 5 min, followed by bending it to 180° under an applied external force. While maintaining the external force, the film was further cooled to room temperature, and the bent angle was measured and recorded as θ_d. Subsequently, the temporarily bent hydrogel film was subjected to 90 °C, and the change in the bending angle (θ_m) was recorded as a function of heating time. The shape edit ratio (R_e) and the shape maintainable ratio (R_m) of PVA/MXene hydrogels were defined by the following eqs 3 and 4:[46]

https://doi.org/10.1021/acsapm.5c03453
ACS Appl. Polym. Mater. 2025, 7, 15659−15670

$$R_e = \frac{\theta_d}{180} \times 100\% \quad (3)$$

$$R_m = \frac{\theta_m}{\theta_d} \times 100\% \quad (4)$$

Notably, both R_e and R_f exceeded 90%, indicating that the polymer underwent permanent remodeling without macroscopic melting. Mechanistically, this was attributed to covalent bond exchange within the polymer network, allowing its topographical rearrangements in response to external forces. Specifically, the shape change occurred without altering chain conformation (or entropy) change, rendering the transformation permanent.[47]

Finite Element Simulation. Using commercial finite-element analysis software ABAQUS/Explicit (version 2022, Simulia, France), the deformation and recovery processes of the composite thin-film material under different external temperatures were studied. Based on the material property parameters of the composite film, a solid homogeneous model was created in Abaqus, incorporating key parameters such as density, thermal expansion coefficient, Young's modulus, and viscoelastic behavior. These material properties were specifically assigned to the cross-petal structure. The global mesh size was set to approximately 0.8 mm, with the element type defined as C3D8I (eight-node linear hexahedral element with reduced integration). Distortion control and hourglass control were enabled to ensure mesh stability. Given the inclusion of the material's viscoelastic properties, a general viscoelastic analysis step was established, with geometric nonlinearity considered. The explicit solver was employed to compute creep, swelling, and viscoelastic integration during the analysis step, with a strain error tolerance of 0.01.

Computational Methods. First, the structure of MXene was optimized by using Gaussian 09 at the B3LYP/6-31G (d) level of theory. Subsequently, the noncovalent interaction (NCI) was calculated using Multiwfn 3.8, and the resulting cube files were then imported into Visual Molecular Dynamics (VMD) to generate Figure 2f. The binding energy between PVA and MXene was determined using the following formula:

$$\Delta E = E(AB) - E(A) - E(B) \quad (5)$$

where $E(AB)$: total energy of the PVA/MXene complex system. $E(A)$ and $E(B)$: energy of the isolated PVA and MXene components.

Measurement of Contraction Force. A 0.5 N load cell was used in the mechanical test system to perform the contraction force. The hydrogel was fixed at one end, while the other end was connected to the test system. The driving force generated during its deformation was recorded by the system (contraction strength; force per unit cross-sectional area).

■ ASSOCIATED CONTENT

Supporting Information

The Supporting Information is available free of charge at https://pubs.acs.org/doi/10.1021/acsapm.5c03453.

The PVA/MXene hydrogel preparation process; SEM and EDS analyses; temperature and NIR effects on hydrogel programming; and actuation performance characterization (PDF)

Spatiotemporal control of shape using NIR light (MP4)

Shape change of adjustable wing thickness (MP4)

Controlled unfolding of solar panels (MP4)

■ AUTHOR INFORMATION

Corresponding Authors

Huaping Wu − *Key Laboratory of Special Purpose Equipment and Advanced Processing Technology, Ministry of Education and Zhejiang Province, College of Mechanical Engineering, Zhejiang University of Technology, Hangzhou 310023, China*; orcid.org/0000-0003-4505-7062; Email: wuhuaping@gmail.com

Aiping Liu − *Zhejiang Key Laboratory of Quantum State Control and Optical Field Manipulation, Department of Physics, Zhejiang Sci-Tech University, Hangzhou 310018, China*; orcid.org/0000-0002-2338-062X; Email: liuaiping1979@gmail.com

Authors

Ping Guo − *Zhejiang Key Laboratory of Quantum State Control and Optical Field Manipulation, Department of Physics, Zhejiang Sci-Tech University, Hangzhou 310018, China*

Jie Zhou − *Key Laboratory of Special Purpose Equipment and Advanced Processing Technology, Ministry of Education and Zhejiang Province, College of Mechanical Engineering, Zhejiang University of Technology, Hangzhou 310023, China*

Chengnan Qian − *Zhejiang Key Laboratory of Quantum State Control and Optical Field Manipulation, Department of Physics, Zhejiang Sci-Tech University, Hangzhou 310018, China*

Wenjie Cao − *Zhejiang Key Laboratory of Quantum State Control and Optical Field Manipulation, Department of Physics, Zhejiang Sci-Tech University, Hangzhou 310018, China*

Yang Yu − *Zhejiang Key Laboratory of Quantum State Control and Optical Field Manipulation, Department of Physics, Zhejiang Sci-Tech University, Hangzhou 310018, China*

Lin Cheng − *Zhejiang Key Laboratory of Quantum State Control and Optical Field Manipulation, Department of Physics, Zhejiang Sci-Tech University, Hangzhou 310018, China*; orcid.org/0000-0001-8680-1383

Daoyou Guo − *Zhejiang Key Laboratory of Quantum State Control and Optical Field Manipulation, Department of Physics, Zhejiang Sci-Tech University, Hangzhou 310018, China*; orcid.org/0000-0002-6191-1655

Complete contact information is available at: https://pubs.acs.org/10.1021/acsapm.5c03453

Author Contributions

P.G.: Methodology, Data curation, Writing-original draft preparation; J.Z.: Data curation, Software, Validation; C.Q.: Data curation, Software; W.C.: Software, Validation; Y.Y.: Software, Validation; D.G.: Software, Validation; L.C.: Formal analysis, Investigation; H.W.: Investigation; A.L.: Supervision, Conceptualization, Methodology, Writing-review and editing.

Notes

The authors declare no competing financial interest.

■ ACKNOWLEDGMENTS

This work was supported by the National Natural Science Foundation of China (Nos. 12272351, 62401509, and 12372168), the National Key Research and Development Program of China (2024YFB3816500), the Zhejiang Provincial Natural Science Foundation of China (Nos. LZ24A020004 and LRG25A020001), the Youth Top-notch Talent Project of Zhejiang Ten Thousand Plan of China (No. ZJWR0308010), and the "Pioneer" and "Leading Goose" R&D Program of Zhejiang (Grant No. 2023C01051).

REFERENCES

(1) Liu, R.; Wang, T.; Li, G.; Fan, Z.; Zhou, Q.; Wang, K.; Li, P.; Huang, W. Self-reinforced hydrogel-based skin-contactable flexible electronics for multimodal electrophysiological signal monitoring and emergency alarming system. *Adv. Funct. Mater.* **2023**, *33* (24), 2214917.

(2) Wang, X.; Zheng, S.; Xiong, J.; Liu, Z.; Li, Q.; Li, W.; Yan, F. Stretch-induced conductivity enhancement in highly conductive and tough hydrogels. *Adv. Mater.* **2024**, *36* (25), 2313845.

(3) Ohm, Y.; Liao, J.; Luo, Y.; Ford, M. J.; Majidi, C. Reconfigurable electrical networks within a conductive hydrogel composite. *Adv. Mater.* **2023**, *35* (14), 2209408.

(4) Li, W.; Liu, J.; Wei, J.; Yang, Z.; Ren, C.; Li, B. Recent progress of conductive hydrogel fibers for flexible electronics: Fabrications, applications, and perspectives. *Adv. Funct. Mater.* **2023**, *33* (17), 2213485.

(5) Li, G.; Li, C.; Li, G.; Yu, D.; Song, Z.; Wang, H.; Liu, X.; Liu, H.; Liu, W. Development of conductive hydrogels for fabricating flexible strain sensors. *Small* **2022**, *18* (5), 2101518.

(6) Wang, Z.; Zhao, T.; Yang, S.; Meng, Y.; Wang, X. Programming Supramolecular Hydrogels by Constructing a Multibranch Selection Structure. *CCS Chem.* **2024**, *6* (8), 1951−1964.

(7) Qian, C. N.; Guo, P.; Wang, R. F.; Luo, X. Z.; Yu, Y.; Cheng, L.; Liu, A. P. Photothermally responsive conductive hydrogels for dual-mode self-sensing soft actuators. *Chem Eng J* **2025**, *519*, 165091.

(8) Luo, X. Z.; Zhang, X.; Ji, S. P.; Wu, C.; Cheng, L.; Guo, D. Y.; Wang, S. L.; Wu, H. P.; Liu, A. P. Fully self-healing dual-mode tactile sensing strategy for object's dimension and surface morphology recognition. *Nano Energy* **2025**, *136*, 110757.

(9) Chen, J.; Liu, F.; Abdiryim, T.; Liu, X. An overview of conductive composite hydrogels for flexible electronic devices. *Adv. Compos. Hybrid Mater.* **2024**, *7* (2), 35.

(10) Zhao, Y.; Lo, C.; Ruan, L.; Pi, C.; Kim, C.; Alsaid, Y.; Frenkel, I.; Rico, R.; Tsao, T.; He, X. Somatosensory actuator based on stretchable conductive photothermally responsive hydrogel. *Sci. Rob.* **2021**, *6* (53), No. eabd5483.

(11) Ma, Y.; Lu, Y.; Yue, Y.; He, S.; Jiang, S.; Mei, C.; Xu, X.; Wu, Q.; Xiao, H.; Han, J. Nanocellulose-mediated bilayer hydrogel actuators with thermo-responsive, shape memory and self-sensing performances. *Carbohyd. Polym.* **2024**, *335*, 122067.

(12) Huang, H.; Cong, H. T.; Lin, Z.; Liao, L.; Shuai, C. X.; Qu, N.; Luo, Y.; Guo, S.; Xu, Q. C.; Bai, H.; Jiang, Y. Manipulation of Conducting Polymer Hydrogels with Different Shapes and Related Multifunctionality. *Small* **2024**, *20* (25), 2309575.

(13) Wu, S. S.; Guo, J.; Wang, Y. L.; Xie, H.; Zhou, S. B. Cryopolymerized polyampholyte gel with antidehydration, self-healing, and shape-memory properties for sustainable and tunable sensing electronics. *ACS Appl. Mater. Interfaces* **2022**, *14* (37), 42317−42327.

(14) Wang, Y.; Ye, H.; He, J.; Ge, Q.; Xiong, Y. Electrothermally controlled origami fabricated by 4D printing of continuous fiber-reinforced composites. *Nat. Commun.* **2024**, *15* (1), 2322.

(15) Diao, S.; Meng, L.; Pelicano, C. M.; Huang, J.; Tian, Z.; Lai, F.; Liu, T.; Cao, S. Rapid photothermal-responsive soft hydrogel actuator contained $Ti_3C_2T_x$ MXene and laponite clay with enhanced mechanical properties. *ACS Appl. Mater. Interfaces* **2024**, *16* (33), 44067−44076.

(16) Zhao, J. X.; Zhai, X. J.; Li, P. Y.; Wang, X. H.; Wen, Y. H.; Xia, W.; Luo, T. Y.; Wu, L. D. From Sea Cucumbers to Soft Robots: A Photothermal-responsive hydrogel actuator with shape memory. *ACS Appl. Mater. Interfaces* **2025**, *17* (4), 6979−6986.

(17) Geng, Q. W.; Zhang, F. H.; Liu, Y. J.; Leng, J. S. Multiple-stimuli response composite hydrogels with high mechanical property and triple shape memory effect. *Compos. Sci. Technol.* **2023**, *242*, 110169.

(18) Xu, D.; Li, Z.; Li, L.; Wang, J. Insights into the photothermal conversion of 2D MXene nanomaterials: Synthesis, mechanism, and applications. *Adv. Funct. Mater.* **2020**, *30* (47), 2000712.

(19) Qian, C. H.; Li, Y. Q.; Liu, L. K.; Chen, C.; Han, L. NIR responsive and conductive PNIPAM/PANI nanocomposite hydrogels with high stretchability for self-sensing actuators. *J. Mater. Chem. C* **2023**, *11* (20), 6741−6749.

(20) Yang, Y.; Tan, Y.; Wang, X. L.; An, W. L.; Xu, S. M.; Liao, W.; Wang, Y. Z. Photothermal nanocomposite hydrogel actuator with electric-field-induced gradient and oriented structure. *ACS Appl. Mater. Interfaces* **2018**, *10* (9), 7688−7692.

(21) Zhang, X.; Chen, L. S.; Zhang, C.; Liao, L. Q. Robust near-infrared-responsive composite hydrogel actuator using Fe/tannic acid as the photothermal transducer. *ACS Appl. Mater. Interfaces* **2021**, *13* (15), 18175−18183.

(22) Dhamodharan, D.; Dhinakaran, V.; Byun, H. S. MXenes: An emerging 2D material. *Carbon* **2022**, *192*, 366−383.

(23) Liu, L.; Mao, Y.; Gao, M.; Fan, X.; Li, Y. Mxene-based hydrogel actuators with swift bidirectional actuation, programmable deformation and self-sensing functionality. *Eur. Polym. J.* **2025**, *240*, 114331.

(24) Liu, L.; Gao, M.; Fan, X.; Lu, Z.; Li, Y. Fast fabrication of stimuli-responsive MXene-based hydrogels for high-performance actuators with simultaneous actuation and self-sensing capability. *J. Colloid Interface Sci.* **2025**, *684*, 469−480.

(25) Cao, H.; Neal, N. N.; Pas, S.; Radovic, M.; Lutkenhaus, J. L.; Green, M. J.; Pentzer, E. B. Architecting MXenes in polymer composites. *Prog. Polym. Sci.* **2024**, *153*, 101830.

(26) Xu, S. M.; Yu, W. J.; Yao, X. L.; Zhang, Q.; Fu, Q. Nanocellulose-assisted dispersion of graphene to fabricate poly(vinyl alcohol)/graphene nanocomposite for humidity sensing. *Compos. Sci. Technol.* **2016**, *131*, 67−76.

(27) Zheng, Y. Q.; Li, Y. L.; Wang, L. L.; Xu, H.; Han, W. A wearable strain sensor based on self-healable MXene/PVA hydrogel for bodily motion detection. *Microelectron. Eng.* **2024**, *291*, 112197.

(28) Miao, X.; Li, Z.; Hou, K.; Gao, Q.; Huang, Y.; Wang, J.; Yang, S. Bioinspired multi-crosslinking and solid-liquid composite lubricating MXene/PVA hydrogel based on salting out effect. *Chem. Eng. J.* **2023**, *476*, 146848.

(29) Eslami, R.; Azizi, N.; Santhirakumaran, P.; Mehrvar, M.; Zarrin, H. 3D dual network effect of alkalinized MXene and hBN in PVA for wearable strain/pressure sensor applications. *Chem. Eng. J.* **2024**, *480*, 148063.

(30) Cheng, R. F.; Wang, J. C.; Hu, T.; Zhao, Y. M.; Liang, Y.; Wang, X. H.; Zhou, Y. C. Stabilizing MXene suspension with polyhydric alcohols. *J. Mater. Sci. Technol.* **2023**, *165*, 219−224.

(31) Wang, W.; Cai, T. J.; Tang, L.; Zhang, J. D.; Du, C.; Tang, J. X.; Yang, Y. Q.; Yin, L.; Kang, H.; Fan, Z. M. Shape-reconfigurable supramolecular MXene-based memory films. *ACS Appl. Nano Mater.* **2023**, *6* (20), 18721−18728.

(32) Luo, X.; Zhu, L.; Wang, Y. C.; Li, J.; Nie, J.; Wang, Z. L. A flexible multifunctional triboelectric nanogenerator based on MXene/PVA hydrogel. *Adv. Funct. Mater.* **2021**, *31* (38), 2104928.

(33) Lu, T.; Chen, F. Multiwfn: A multifunctional wavefunction analyzer. *J. Comput. Chem.* **2012**, *33* (5), 580−592.

(34) Guo, X. R.; Sheng, P. H.; Hu, J. W.; Liu, J.; Wang, S. L.; Ma, Q.; Yu, Z. Z.; Ding, Y. Multistimuli-responsive shape-memory composites with a water-assisted self-healing function based on sodium carboxymethyl cellulose/poly(vinyl alcohol)/MXene. *ACS Appl. Mater. Interfaces* **2024**, *16* (14), 17981−17991.

(35) Zhou, C.; Zhao, X. H.; Xiong, Y. S.; Tang, Y. H.; Ma, X. T.; Tao, Q.; Sun, C. M.; Xu, W. L. A review of etching methods of MXene and applications of MXene conductive hydrogels. *Eur. Polym. J.* **2022**, *167*, 111063.

(36) Liu, H.; Du, C.; Liao, L.; Zhang, H.; Zhou, H.; Zhou, W.; Ren, T.; Sun, Z.; Lu, Y.; Nie, Z.; et al. Approaching intrinsic dynamics of MXenes hybrid hydrogel for 3D printed multimodal intelligent devices with ultrahigh superelasticity and temperature sensitivity. *Nat. Commun.* **2022**, *13* (1), 3420.

(37) Yang, T. Y.; Wang, M.; Jia, F.; Ren, X. Y.; Gao, G. H. Thermo-responsive shape memory sensors based on tough, remolding and anti-freezing hydrogels. *J. Mater. Chem. C* **2020**, *8* (7), 2326−2335.

https://doi.org/10.1021/acsapm.5c03453
ACS Appl. Polym. Mater. 2025, 7, 15659−15670

(38) Cai, G.; Wang, J.; Qian, K.; Chen, J.; Li, S.; Lee, P. S. Extremely stretchable strain sensors based on conductive self-healing dynamic cross-links hydrogels for human-motion detection. *Adv. Sci.* **2016**, *4* (2), 1600190.
(39) Wang, Y.; Zhang, Z. H.; Chen, H. X.; Zhang, H.; Zhang, H.; Zhao, Y. J. Bio-inspired shape-memory structural color hydrogel film. *Sci. Bull.* **2022**, *67* (5), 512−519.
(40) Li, Z.; Li, Z.; Zhou, S.; Zhang, J.; Zong, L. Biomimetic multiscale oriented PVA/NRL hydrogel enabled multistimulus responsive and smart shape memory actuator. *Small* **2024**, *20* (25), 2311240.
(41) Ma, Y.; Hua, M.; Wu, S.; Du, Y.; Pei, X.; Zhu, X.; Zhou, F.; He, X. Bioinspired high-power-density strong contractile hydrogel by programmable elastic recoil. *Sci. Adv.* **2020**, *6* (47), No. eabd2520.
(42) Lu, J. L.; Jia, J. P.; Xu, Q.; Zhang, J. W. Molecular hydrophilicity-accelerated shape memory hydrogels with integrated sensing performance. *Macromolecules* **2025**, *58* (17), 9151−9162.
(43) Hai, N.; Lu, J.; Li, Y.; Wang, Y.; Zhang, J. Poly(n-isopropylacrylamide) microgel containing hydrogel enables cooling/water induced shape recovery and transient image display. *ACS Appl. Polym. Mater.* **2025**, *7* (11), 7303−7310.
(44) Chen, C.; Zhao, X. K.; Chen, Y. J.; Chu, W. S.; Wu, Y. X.; Zhao, Y. S.; Shi, P. J.; Chen, W. Z.; Li, H.; He, X. M.; Liu, H. Z. Photoinduced dual shape programmability of covalent adaptable networks with remarkable mechanical properties. *Nano Lett.* **2022**, *22* (21), 8413−8421.
(45) Zheng, N.; Fang, Z. Z.; Zou, W. K.; Zhao, Q.; Xie, T. Thermoset shape-memory polyurethane with intrinsic plasticity enabled by transcarbamoylation. *Angew. Chem. Int. Ed.* **2016**, *55* (38), 11421−11425.
(46) Zhao, Q.; Zou, W.; Luo, Y.; Xie, T. Shape memory polymer network with thermally distinct elasticity and plasticity. *Sci. Adv.* **2016**, *2* (1), No. e1501297.
(47) Ni, C. J.; Chen, D.; Yin, Y.; Wen, X.; Chen, X. L.; Yang, C.; Chen, G. C.; Sun, Z.; Wen, J. H.; Jiao, Y. R.; Wang, C. Y.; Wang, N.; Kong, X. X.; Deng, S. H.; Shen, Y. Q.; Xiao, R.; Jin, X. M.; Li, J.; Kong, X. Q.; Zhao, Q.; Xie, T. Shape memory polymer with programmable recovery onset. *Nature* **2023**, *622* (7984), 748−753.

https://doi.org/10.1021/acsapm.5c03453
ACS Appl. Polym. Mater. 2025, 7, 15659−15670